



Published in final edited form as:

*Cell Rep.* 2013 July 11; 4(1): . doi:10.1016/j.celrep.2013.05.041.

## Checkpoint Kinases Regulate a Global Network of Transcription Factors in Response to DNA Damage

Eric J. Jaehnig<sup>1,2,3</sup>, Dwight Kuo<sup>4</sup>, Hans Hombauer<sup>1,2,3</sup>, Trey G. Ideker<sup>2,4,5,6</sup>, and Richard D. Kolodner<sup>1,2,3,5,6,\*</sup>

<sup>1</sup>Ludwig Institute for Cancer Research, University of California School of Medicine, San Diego, 9500 Gilman Drive, La Jolla, CA 92093, USA

<sup>2</sup>Department of Medicine, University of California School of Medicine, San Diego, 9500 Gilman Drive, La Jolla, CA 92093, USA

<sup>3</sup>Department of Cellular and Molecular Medicine, University of California School of Medicine, San Diego, 9500 Gilman Drive, La Jolla, CA 92093, USA

<sup>4</sup>Department of Bioengineering, University of California School of Medicine, San Diego, 9500 Gilman Drive, La Jolla, CA 92093, USA

<sup>5</sup>UCSD Moores Cancer Center, University of California School of Medicine, San Diego, 9500 Gilman Drive, La Jolla, CA 92093, USA

<sup>6</sup>Institute of Genomic Medicine, University of California School of Medicine, San Diego, 9500 Gilman Drive, La Jolla, CA 92093, USA

### SUMMARY

DNA damage activates checkpoint kinases that induce several downstream events, including widespread changes in transcription. However, the specific connections between the checkpoint kinases and downstream transcription factors (TFs) are not well understood. Here, we integrate kinase mutant expression profiles, transcriptional regulatory interactions, and phosphoproteomics to map kinases and downstream TFs to transcriptional regulatory networks. Specifically, we investigate the role of the *Saccharomyces cerevisiae* checkpoint kinases (Mec1, Tel1, Chk1, Rad53, and Dun1) in the transcriptional response to DNA damage caused by methyl methanesulfonate. The result is a global kinase-TF regulatory network in which Mec1 and Tel1 signal through Rad53 to synergistically regulate the expression of more than 600 genes. This network involves at least nine TFs, many of which have Rad53-dependent phosphorylation sites, as regulators of checkpoint-kinase-dependent genes. We also identify a major DNA damage-induced transcriptional network that regulates stress response genes independently of the checkpoint kinases.

---

© 2013 The Authors

\*Correspondence: rkolodner@ucsd.edu.

This is an open-access article distributed under the terms of the Creative Commons Attribution-NonCommercial-No Derivative Works License, which permits non-commercial use, distribution, and reproduction in any medium, provided the original author and source are credited.

### ACCESSION NUMBERS

The GEO accession number for the microarray data reported in this paper is GSE40351.

### SUPPLEMENTAL INFORMATION

Supplemental Information includes Extended Experimental Procedures, ten figures, and ten tables and can be found with this article online at <http://dx.doi.org/10.1016/j.celrep.2013.05.041>.

## INTRODUCTION

DNA damage can be caused by exogenous agents, such as carcinogens and ionizing radiation, and by endogenous agents, such as reactive oxidative species. This can result in errors during DNA replication or blockage of the replication machinery, leading to mutations or genomic rearrangements. Cellular function or viability may be impaired if the resulting mutations or genomic rearrangements affect critical genes. In addition, alteration of genes with roles in cellular homeostasis, such as control of the cell cycle, cell migration, or cellular adhesion, may contribute to the development of cancer (Branzei and Foiani, 2009; Kolodner et al., 2002).

Response mechanisms that recognize DNA damage are well conserved in eukaryotes. The DNA damage response (DDR) involves a signal transduction cascade in which recognition of DNA damage activates checkpoint kinases from the PI3K-like family, particularly ataxia telangiectasia mutated (ATM) and ATM/Rad3 related (ATR) (Mec1 and Tel1 in *S. cerevisiae*; see Figure 1A). ATM and ATR then phosphorylate Chk family checkpoint kinases, including Chk1 and Chk2 (Chk1 and Rad53 in *S. cerevisiae*; Rad53 also phosphorylates a third checkpoint kinase, Dun1), but the relative importance of each checkpoint kinase to the DDR depends on the type of DNA damage. The activated checkpoint kinases phosphorylate numerous effector proteins that regulate multiple cellular processes, including cell-cycle progression, DNA replication and repair, and, in multicellular organisms, apoptosis (Branzei and Foiani, 2006; Putnam et al., 2009; Rouse and Jackson, 2002).

Activation of the checkpoint kinases also induces changes in expression of hundreds to thousands of genes in *S. cerevisiae* (Gasch et al., 2001; Putnam et al., 2009; Workman et al., 2006). In one example, the transcription factor (TF) Rfx1/Crt1 represses multiple targets, including the ribonucleotide reductase genes (*RNR2*, *RNR3*, and *RNR4*), *HUG1*, and *RFX1* itself (Figure 1A) (Basrai et al., 1999; Huang et al., 1998). Following DNA damage, repression is relieved by hyperphosphorylation of Rfx1 by Dun1 (Huang et al., 1998). Interestingly, most of the genes that are differentially expressed in response to DNA damage are not involved in DNA repair but rather act in other processes such as cell-cycle progression, environmental stress responses, protein homeostasis, and energy metabolism (Gasch et al., 2001; Putnam et al., 2009). For example, Rad53 phosphorylates and potentially represses Swi6, a TF that drives expression of genes that promote cell-cycle progression from G1 to S phase (Sidorova and Breeden, 1997, 2003).

Previously, we used genome-wide chromatin immunoprecipitation (ChIP) and TF mutant expression profiling to map transcriptional networks underlying the DDR induced by methyl methanesulfonate (MMS) in *S. cerevisiae* (Workman et al., 2006). These data have since been combined with data from other high-throughput studies to identify potential transcriptional targets for most known *S. cerevisiae* TFs (Beyer et al., 2006). Here, we integrate this transcriptional network with gene expression profiles of checkpoint kinase mutants to map interactions between kinases and TFs during the DDR. We further explored kinase-TF interactions using mass spectrometry to identify checkpoint-kinase-dependent phosphorylation sites on candidate TFs. We found that the checkpoint-kinase-mediated transcriptional response is more complex than previously appreciated. Specifically, activation of Rad53 in a manner dependent on Mec1 and, to a greater extent than other MMS-induced checkpoint responses, on Tel1 plays a central role in inducing a transcriptional network that involves both Dun1-dependent and Dun1-independent branches. In addition, we identified transcriptional networks induced by DNA damage independently of the checkpoint kinases.

## RESULTS

### Rad53 Is the Central Regulator of the Checkpoint- Kinase-Dependent Transcriptional Response to DNA Damage

We analyzed the mRNA expression profiles of *S. cerevisiae* before and after exposure to MMS in wild-type (WT) cells and in checkpoint kinase single and double mutants (strains shown in Figure 1A and Table S1; expression profile data shown in Table S2).

Approximately 1,700 genes showed significant expression changes during the DDR in WT cells (Table S3). As shown in Figure 1B, differential expression of a number of genes was attenuated by deletion of *MEC1*, *RAD53*, or *DUN1*. In contrast, deletion of *STE11*, a kinase that mediates the pheromone response during mating (Bardwell, 2004), did not substantially affect DNA damage-induced changes in gene expression (Figure 1B; Table S3).

Hierarchical clustering of the WT and mutant differential expression profiles revealed high-level insights into their regulatory relationships (Figure 1C). In the resulting tree, the distance between two strains reflects the difference between the expression profiles of the strains, and the distance of a strain from WT indicates the severity of its defect in the transcriptional response to MMS (Ideker et al., 2001; Van Driessche et al., 2005). For instance, *chk1Δ* clustered closely with WT, *chk1Δdun1Δ* clustered with *dun1Δ*, and *chk1Δrad53Δ* clustered with *rad53Δ*, suggesting that Chk1 does not contribute significantly to the transcriptional response to MMS. The expression profile of *rad53Δdun1Δ* was similar to that of *rad53Δ* and distinct from that of *dun1Δ*, and the expression profile of the *dun1Δ* mutant was much closer to WT than that of the *rad53Δ* mutant, consistent with Dun1 acting downstream of Rad53 and with a larger fraction of the transcriptional response being mediated by Rad53 than by Dun1 (Figure 1C) (Allen et al., 1994; Bashkirov et al., 2003). The distance between the WT and *mec1Δ* expression profiles confirmed that Mec1 plays an important role in regulating the transcriptional response to MMS (Gasch et al., 2001). A *tel1Δ* mutation resulted in only minor defects in the MMS-induced expression profile. However, the *mec1Δtel1Δ* double mutant affected the transcriptional response to a much greater extent than *mec1Δ*. Finally, the *mec1Δtel1Δ* and *rad53Δ* mutants had differential expression profiles that showed similar defects, supporting the model that Mec1 and Tel1 converge on Rad53 to regulate the checkpoint-kinase-dependent branch of the transcriptional response (Figure 1D).

### Implicating Downstream TFs in the Checkpoint-Kinase- Dependent Transcriptional Response

To map the transcriptional network induced by the checkpoint kinases, we first identified the genes whose DNA damage-induced transcriptional response was dependent on each kinase. Figure 2A illustrates this for a subset of genes in the *dun1Δ* experiment: *HUG1* and *RNR3* are targets of the Rfx1 TF, which is regulated by Dun1 (Figure 1A) (Basrai et al., 1999; Huang et al., 1998). Both *HUG1* and *RNR3* were upregulated by MMS in the WT strain but showed a reduced response in the *dun1Δ* mutant (Figure 2A). Similarly, *ADE4* and *HOF1* were downregulated in WT but not in the *dun1Δ* mutant. We refer to these genes as “kinase dependent” because they require the kinase for full differential expression during the DDR.

By evaluating genes for statistically significant reductions in differential expression in each of the kinase mutants (Table S2; Table S4 lists the kinase dependencies and other properties for all genes included in the expression analysis), we identified 109 and 146 genes that were dependent on Dun1 and Mec1, respectively (Figure 2B; Table S3). Many more genes were dependent on Rad53 (~600 genes), providing an estimate for the number of checkpoint-kinase-dependent genes. Consistent with the model in which Dun1 regulates Rfx1, this analysis revealed that 41 genes, including known Rfx1 targets (*FSH3*, *HUG1*, *RNR2*, *RNR3*,

and *RNR4*), showed a reduction in differential expression in the *rfx1Δ* mutant and that 16 and 39 of these showed reduced differential expression in *dun1Δ* and *rad53Δ* mutants, respectively (Tables S4 and S5) (Basrai et al., 1999; Huang et al., 1998).

Using a previously defined TF regulatory network comprising approximately 13,000 TF-target gene interactions for 158 TFs (Beyer et al., 2006), we identified TFs whose targets showed significant enrichment for kinase-dependent genes (Figure 3A; Table S6). In these cases, the kinase was inferred to mediate expression of the target genes by regulating the activity of that TF during the DDR. Figure 3B shows the network inferred for the set of Dun1-dependent genes. We found significant enrichment for targets of Rfx1 in both the Dun1- and Rfx1- dependent gene sets, confirming that Rfx1 regulates predicted Rfx1 targets and lies downstream of Dun1 (Figure 3B; Table S6). The combined network for TFs consistently inferred from all of the checkpoint kinase-dependent gene sets contained interactions between the checkpoint kinases and nine downstream TFs (Figures 3C, S1, and S2). Analysis of previously published expression data indicated that mutations in the nonessential TF genes (*MSN4*, *MBP1*, *SWI6*, *SWI4*, *GCN4*, *RFX1*, and *FKH2*) reduced expression of many MMS-induced genes whose expression was similarly affected by deletion of *RAD53* (Figures S3, S4, and S5) (Workman et al., 2006). In addition, the checkpoint kinases showed significant potential interactions with seven other TFs (Arg81, Cad1, Fkh1, Gln3, Hir2, Msn2, and Rph1), albeit with less consistency (Figure S1; Table S6).

GO enrichment analysis of the Rad53-dependent genes predicted to be targets of each TF in the Dun1-regulated branch of this network revealed that these TFs regulate genes involved in DNA metabolism (Rfx1), amino acid metabolism (Gcn4), cell division (Fkh2, Mcm1, and Ndd1), and rRNA processing (Fkh2 and Ndd1) (Figures 3C, S1, and S2; Table S7). These observations are consistent with previous studies implicating Rfx1 in nucleotide metabolism during the DDR (Huang et al., 1998), Gcn4 in stress responses induced by environmental amino acid imbalances (Hinnebusch and Fink, 1983; Yoon et al., 2004), and the complex containing Fkh2, Mcm1, and Ndd1 in promoting the G2 to M cell-cycle transition (Bähler, 2005). The network of TFs controlled by the checkpoint kinases (Figure 3C) did not include the Arg81, Rtg3, and Cad1 TFs shown in Figure 3B because enrichment of their targets was not consistently observed in the other checkpoint kinase mutants (Table S6). However, all the target genes that allowed us to infer connections for Dun1 with Arg81 and Rtg3 were also included in the set of Gcn4 targets (Figure 3B), suggesting that a limitation of this approach is that we cannot determine the specificity of TFs whose targets have a high degree of overlap. Finally, only 43% of the Dun1-dependent genes (47 out of 109) were included in this network (Figures 2C and 3B), indicating that Dun1 may also regulate other TFs that we could not identify using this approach.

The TFs acting downstream of Rad53, but not Dun1, included Msn4, which regulates responses to stress and temperature, and MBF (Swi6-Mbp1) and SBF (Swi6-Swi4), which regulates G1 to S transition in the cell cycle and expression of nucleic acid metabolism genes involved in DNA replication and repair (Figures 3C and S2; Table S7) (Sidorova and Breeden, 1993; Verma et al., 1992). At a lower threshold, enrichment for targets of Arg81, Rtg3, and Cad1 (also regulated by Dun1) and of Fkh1, Gln3, Hir2, and Msn4 and Rph1 (Dun1 independent) was also observed (Figure S1; Table S7). In summary, our analysis reveals a global transcriptional regulatory network in which Rad53 regulates at least Msn4 and the SBF/MBF complexes independently of Dun1 and Rfx1, Gcn4, and the Fkh2/Mcm1/Ndd1 complex via Dun1 (Figure 3C).

## Rad53-Dependent Phosphorylation of TFs in the Checkpoint-Kinase-Mediated Response

To determine if the checkpoint kinase cascade regulates the TFs identified in this global network (Figure 3C) via phosphorylation, we used mass spectroscopy (MS) to compare the levels of phosphopeptides for each TF purified from a *rad53Δ* mutant with those same peptides purified from an isogenic WT strain (Figure 4; Table S8). (Rfx1 was not examined because its phosphoregulation by Rad53 and Dun1 has been described by Huang et al. (1998). Also note that Rph1, an additional TF included in Figure S1, has been shown to undergo Rad53-dependent, DNA damage-induced phosphorylation (Kim et al., 2002).) The *rad53Δ* mutant was the focus of this analysis because virtually the entire checkpoint-kinase-mediated transcriptional response to MMS was Rad53 dependent (Figures 1C and 3C). Because a single phosphosite was often seen in multiple peaks/peptides, we also calculated the total relative levels for all MS peaks containing a given phosphosite to better determine the extent to which phosphorylation was affected by the *rad53Δ* mutation (Table 1).

We observed peptides with Rad53-dependent changes in phosphorylation from all eight TFs tested. In total, 34 phosphorylation sites (greater phosphorylation in WT) and 21 dephosphorylation sites (greater phosphorylation in the *rad53Δ* mutant) were observed in at least one of three independent experiments conducted for each TF (Figure 4). Ndd1, Msn4, Fkh2, Mbp1, and Swi6 had at least one site that showed a net reduction in phosphorylation in the *rad53Δ* mutant in at least two experiments (Table 1), whereas Gcn4, which may also be activated by the accumulation of unspliced mRNAs in response to DNA damage (Ghavidel et al., 2007), and Swi4 had sites showing a net reduction in phosphorylation in only one experiment. The only potential Rad53-dependent phosphorylation site on Mcm1 showed inconsistent results in different experiments (Table 1). Fkh2, Msn4, Ndd1, Mbp1, and Swi6 also had sites showing a net increase in phosphorylation in *rad53Δ* mutants in at least one experiment (Table 1), possibly due to activation of a phosphatase or inactivation of an intermediate kinase by Rad53. Fkh2, Mcm1, or Ndd1 activity may also be indirectly regulated by Hcm1, a transcriptional activator not included in the database we used to identify the TFs (Pramila et al., 2006). However, it is unlikely that Hcm1 plays a role in the regulation of these TFs because *HCM1* gene expression did not change in WT and was actually repressed by MMS treatment in *rad53Δ* mutants that failed to downregulate targets of Fkh2, Mcm1, and Ndd1 (Table S2). Interestingly, a single peptide on Swi6 contained six potential phosphorylation sites that could be separated into two groups. Peptides containing T169 and S170 showed Rad53-dependent phosphorylation, whereas peptides containing S176, S178, T179, and T182 (but not T169 or S170) were found either to not be changing or to show Rad53-dependent dephosphorylation when peptides with phosphorylation of multiple sites were observed (Figure 4; Table 1). Furthermore, we observed higher levels of peptides containing T169 or S170 in WT yeast treated with MMS compared to untreated yeast, whereas peptides containing only S176, S178, T179, and/or T182 were not induced by MMS (data not shown). MMS also induced phosphorylation of Rad53-dependent sites on Swi4 (S271) and Mbp1 (S133, S191, and S212).

Putative Rad53 consensus sites accounted for 17 of the 34 potential Rad53-dependent phosphorylation sites, including T169 and S170 on Swi6, S212 on Mbp1, and S271 on Swi4 (Table 1) (Sidorova and Breeden, 2003; Smolka et al., 2007). Meanwhile, only 2 of the 34 sites were Mec1/Tel1 consensus sites (Kim et al., 1999), only 2, which were also Rad53-dependent phosphorylation sites on Ndd1 and Mbp1, were Dun1 consensus sites, and only 1, which was also a Rad53-dependent site on Fkh2, was a Cdc28 consensus site (Sanchez et al., 1997; Songyang et al., 1994). Although the Dun1-dependent set of genes was enriched for targets of Gcn4, Fkh2, and Mcm1, we did not observe phosphorylation of Dun1 consensus phosphorylation sites on these TFs. These observations may reflect the fact that Rad53 and Dun1 consensus sites are not yet well defined. Regardless of whether

phosphoregulation of these TFs occurs directly by Rad53 or Dun1 or indirectly by downstream kinases or phosphatases, it appears that nearly all of the TFs have Rad53-dependent phosphorylation sites that could contribute to transcriptional regulation.

### **Predicted G1 Targets of MBF Are Activated by MMS, whereas G2/M Targets of Fkh2/Mcm1/Ndd1 Are Repressed by Dun1 Independently of Cell-Cycle Arrest**

Several of the TFs identified regulate cell-cycle progression (Bähler, 2005; Koch et al., 1993; Sidorova and Breeden, 1993; Verma et al., 1991). We, therefore, utilized the results of a previous analysis of cell-cycle-specific gene expression (Spellman et al., 1998) to investigate the relationship of the checkpoint-kinase-dependent transcriptional response to the cell cycle. As shown in Figure 5A and Table S9, the set of Rad53-dependent genes upregulated by MMS treatment was enriched for genes with peak expression in G1 phase, whereas the downregulated set was enriched for genes with peak expression in S, G2, and M phases. Specifically, G1-specific genes included upregulated genes predicted to be targets of Mbp1, Swi4, and Swi6, whereas G2/M phase genes included downregulated targets of Fkh2, Ndd1, and Mcm1 (Figure 5B; Table S9).

Previous studies have suggested two distinct models for how Rad53 regulates Swi6 during the DDR. Rad53 may inhibit expression of Swi6 target genes and, thus, cell-cycle progression (Sidorova and Breeden, 1997, 2003). Alternatively, Rad53 may activate the Mbp1/Swi6 (MBF) complex in response to DNA damage (Bastos de Oliveira et al., 2012; Travesa et al., 2012). In the network of putative Mbp1, Swi4, and Swi6 targets regulated by Rad53 (Figure 5C), the majority of Mbp1 target genes were upregulated during the MMS response. Taken together with the observation that the upregulated targets of Mbp1 and Swi6 were enriched for G1-specific genes (Figure 5B; Table S9), our results are consistent with the model in which Rad53 activates transcription by MBF in response to DNA damage. Furthermore, our GO enrichment analysis suggests that Rad53 most likely activates expression of MBF target genes involved in DNA replication and repair (Figures 3B and S2). However, just over half of the predicted targets (17 out of 31) of Swi4 and/or Swi6, but not Mbp1, were downregulated by MMS (Figure 5C), and downregulated targets of these TFs showed enrichment for G2/M genes (Figure 5B; Table S9). These results suggest that the Swi4/Swi6 (SBF) complex may play a different role in the transcriptional response to MMS treatment.

Of the remaining TFs in the checkpoint-kinase-dependent network (Figure 3C), only Fkh2, Mcm1, and Ndd1, which are also targets of Dun1, showed enrichment for cell-cycle-specific gene expression (Figure 5B; Table S9). Putative downregulated targets of all three of these TFs showed enrichment for G2/M genes, including *CDC5*, *CLB2*, *ACE2*, and *SWI5* (Figure 3B; Tables S4 and S9). Although deletion of *FKH2* affected expression of a small set of genes that was primarily upregulated by MMS (Figure S3), regulation of Mcm1 and Ndd1, the essential members of the complex, by the checkpoint kinases may be sufficient for mediating repression of G2/M targets.

Under the conditions used here, MMS causes a cell-cycle delay in S phase (the intra-S checkpoint; Figures 5D and S6) (Paulovich and Hartwell, 1995). This raises the question of whether repression of genes associated with the G2 to M phase transition was due to indirect effects associated with a greater proportion of cells residing in S phase during MMS treatment. As shown in Figure 5D, asynchronous populations of WT cells analyzed by fluorescence-activated cell sorting (FACS) were evenly distributed between cells with either 1 N or 2 N DNA content. However, MMS treatment resulted in a shift toward a greater population with 1 N DNA content and the appearance of a population of cells with S phase DNA content between 1 N and 2 N (Figure 5D). By contrast, the *rad53Δ* mutant strains were deficient in this checkpoint because MMS-treated *rad53Δ* mutant cells resembled untreated

cells (Figures 5D and S6). Both the *mec1Δ* and *mec1Δtel1Δ* mutant strains also displayed this checkpoint defect, but the *dun1Δ* and *dun1Δchk1Δ* mutants had an intact intra-S checkpoint (Figures 5D and S6). Consistent with these results, release of α factor-arrested cells into MMS resulted in a delay in progression through S phase in both the *dun1Δ* mutant and WT, whereas the *rad53Δ* strain progressed rapidly through S phase (data not shown).

The observation that a *dun1Δ* deletion mutant arrests in S phase in response to MMS treatment (Figure 5D) even though deletion of *DUN1* prevented DNA damage-induced repression of predicted Fkh2, Mcm1, and Ndd1 targets with peak expression in G2/M (Figure S3) suggests that these genes are not repressed in WT cells as a result of DNA damage-induced cell-cycle arrest. Rather, Dun1 likely directly regulates DNA damage-induced repression of these genes by modulating the activity of the transcriptional complex consisting of Mcm1, Ndd1, and possibly Fkh2. Consistent with this, the expression profiles of *mec1Δ* and *dun1Δ* clustered together (Figure 1B), and the sets of Mec1- and Dun1-dependent genes overlapped by ~50% (Table S5) even though deletion of *MEC1* and *DUN1* resulted in a defect (no cell-cycle delay) and no defect in the intra-S checkpoint (cell-cycle delay) in response to MMS, respectively. However, the majority of Mcm1 and Ndd1 targets and approximately half of the predicted Fkh2 targets showed stronger defects in differential expression in the *rad53Δ* mutant than in the *dun1Δ* mutant (Figure S3). This may reflect a failure to arrest in response to MMS that leads to a higher proportion of cells expressing G2/M genes and/or an additional role for Rad53 in the direct regulation of these TFs. Consistent with the latter possibility, the most likely checkpoint-kinase-dependent phosphorylation sites on Fkh2 (S596) and Ndd1 (S454) were consensus sites for Rad53 (Table 1). In addition, most of the Rfx1 and Gcn4 targets showing differential expression in response to MMS treatment were affected more substantially by deletion of *RAD53* than by deletion of *DUN1* even though they did not show cell-cycle-specific gene expression (Figure S4). Finally, deleting *TEL1* in a *mec1Δ* mutant resulted in reduced DNA damage-induced regulation of many additional genes even though the *mec1Δ* mutation was sufficient to cause a complete defect in MMS-induced cell-cycle delay (Figures 2B and 5D). These observations suggest that the broad role that Rad53 plays in regulating transcription in response to MMS is not solely a consequence of cell-cycle arrest.

### A Network of TFs Mediates Gene Expression Independently of the Checkpoint Kinases

Although nearly 1,700 genes were differentially expressed in response to MMS, only ~600 of these showed significantly reduced differential expression in the *rad53Δ* mutant, suggesting a substantial transcriptional response that is checkpoint kinase independent. Therefore, we evaluated the set of differentially expressed genes that was not checkpoint kinase dependent for enrichment of putative TF targets. The differentially expressed genes were divided into a checkpoint-kinase-dependent set of 547 genes (224 genes with expression disrupted in only one of the nine kinase mutants were excluded) and a checkpoint-kinase-independent set of 901 genes, and enrichment for TF targets was computed for each set (Figure 6A; Table S10). We observed enrichment for predicted targets of 18 TFs in the checkpoint-kinase-dependent set and enrichment for targets of 10 different TFs (Cad1, Hsf1, Hap1, Hap4, Rcs1, Rds1, Rpn4, Yap1, and Yap7; Sut1 was of borderline significance) in the checkpoint-kinase-independent set (Figure 6A). Targets of Cad1 (Yap2) were also overrepresented among the Dun1-dependent genes (Figure 3B), but nearly all of the checkpoint-kinase-independent targets of Cad1 were also targets of Yap1 and Yap7 (Figure S7). Thus, there is a strong possibility that Yap1 and/or Yap7 mediates expression of these targets and that Cad1 was implicated in the checkpoint-kinase-independent response to MMS simply because it shares predicted target genes. Similarly, most of the predicted targets of Rds1 were also targets of either Hap1 or Yap1 and Yap7 (Figure S7). Although many predicted targets of Hap1 were also predicted targets of Hap4,

and whereas Yap1 and Yap7 share several common predicted targets, unique predicted targets of each of these TFs were also checkpoint kinase independent (Figure S7). In total, 294 of the 901 checkpoint-kinase-independent genes were predicted targets of Cad1, Hsf1, Hap1, Hap4, Rcs1, Rds1, Rpn4, Sut1, Yap1, or Yap7.

To confirm the role of these TFs in the checkpoint-kinase-independent transcriptional response, we analyzed previously published expression profiles of *rpn4Δ* and *yap1Δ* mutants (Workman et al., 2006) and performed expression profiling of five other TFs (Hap1, Hap4, Rcs1, Sut1, and Yap7; Cad1 and Rds1 were not included because their predicted targets are likely regulated by other TFs, and Hsf1 was not included because it is essential) and found that these TFs all regulated check-point-kinase-independent genes (Figures 6B, S8, S9, and S10). Interestingly, all of these TFs were also found to regulate checkpoint-kinase-dependent genes (Figure 6B) even though the Beyer et al. (2006) analysis only predicted that 16 of the 264 kinase-dependent genes affected by deletion of the TFs were targets of the corresponding TFs.

GO enrichment analysis indicated that these TFs regulate stress response genes. Analysis of both predicted TF target genes in the checkpoint-kinase-independent DDR network (Figure S7) and of TF-dependent gene sets (Figure 6B) indicated that Rcs1 and Yap1 activate and Hap1 represses genes involved in the oxidative stress response (Table S7). Analysis of predicted TF targets in the checkpoint-kinase-independent network also suggested that Hsf1 activates temperature response genes, Rpn4 activates genes regulating proteolysis, and Hap4 represses nucleotide metabolism genes (Figure S7). Given that differential expression of these genes was observed in both cells arrested at the intra-S checkpoint (WT and *dun1Δ* mutant, Figure 5D) and in cells that were checkpoint defective (*rad53Δ* and *mec1Δ* mutants, Figure 5D), it is unlikely that differential expression of these genes was a consequence of a shift in the proportion of cells from one stage of the cell cycle to another in response to MMS treatment.

## DISCUSSION

Here, we integrated data generated using genomic and proteomic approaches to characterize the function of the checkpoint kinases in the transcriptional response induced by DNA damage. Our studies documented a number of key results.

1. Tel1 was dispensable for the transcriptional response elicited by MMS, whereas simultaneous deletion of both *MEC1* and *TEL1* had a far greater effect than deletion of *MEC1* alone even though deletion of *MEC1* causes a complete defect in the cell-cycle delay induced by MMS.
2. Deletion of *RAD53* affected the MMS-induced transcriptional response to the same extent as codeletion of *MEC1* and *TEL1*.
3. Rad53 and Mec1/Tel1 similarly mediated differential expression of ~500 genes, of which ~100 and ~150 were also regulated by Dun1 and Mec1, respectively. These checkpoint-kinase-dependent genes included targets of a set of nine TFs, at least five of which were phosphorylated in a Rad53-dependent fashion.
4. A distinct group of at least seven TFs regulates differential gene expression in response to MMS independently of the checkpoint kinase cascade.
5. The transcriptional response does not appear to be the indirect consequence of perturbation of the cell cycle by MMS.

These results indicate that the MMS-induced transcriptional response involves a considerably more complex network than previously appreciated.



Previous studies have shown that overexpression of *TEL1* can suppress and deletion of *TEL1* can modestly enhance the DNA damage sensitivity of a *mec1Δ* mutant, suggesting that Mec1 and Tel1 have similar activities (Morrow et al., 1995). However, the checkpoint response to MMS, as assessed by MMS-induced S phase delay and inhibition of nuclear division, is entirely dependent on Mec1 (Paulovich and Hartwell, 1995). Furthermore, MMS-induced phosphorylation of Rad53 is almost entirely dependent on Mec1; only a very low level of residual MMS-induced phosphorylation of Rad53 was seen in a *mec1* mutant, and this phosphorylation appeared to be Tel1 dependent (Sanchez et al., 1996). In the gene expression analysis reported here, deletion of *TEL1* had little effect on MMS-induced gene expression, whereas the *mec1Δtel1Δ* double mutant affected differential expression to a much greater extent than the *mec1Δ* single mutant. Mec1 and Tel1 primarily appeared to activate Rad53 because the *rad53Δ* mutants had differential gene expression profiles that were similar to that of the *mec1Δtel1Δ* double mutant. Deletion of *CHK1* did not affect MMS-induced gene expression, consistent with observations that Chk1 is primarily involved in the G2/M checkpoint, whereas MMS, under the conditions used here, primarily activates the intra-S checkpoint (Liu et al., 2000; Paulovich and Hartwell, 1995; Sanchez et al., 1999). Interestingly, deletion of *DUN1*, which acts downstream of Rad53 (Allen et al., 1994; Bashkirov et al., 2003), did not affect differential expression of targets of TFs in the Dun1 branch of the transcriptional response to the same extent that the *rad53Δ* mutation did (Figures S3, S4, and S5). This suggests that Rad53 also acts on Rfx1, Fkh2, Mcm1, Ndd1, and Gcn4 in a Dun1-independent manner. In contrast, Rad53 appears to regulate expression of targets of Msn4, Swi6, Swi4, and Mbp1 through Dun1-independent mechanisms, consistent with previous results showing that SBF (Swi4/Swi6) and MBF (Mbp1/Swi6) are directly regulated by Rad53 (Bastos de Oliveira et al., 2012; Sidorova and Breeden, 1997, 2003; Travesa et al., 2012). Overall, our results show that the MMS-induced checkpoint-kinase-dependent transcriptional response is primarily mediated by activation of Rad53 by Mec1 and Tel1 leading to the activation of downstream Dun1-dependent and Dun1-independent branches. This transcriptional response is far more dependent on Tel1 than MMS-induced cell-cycle delay or Rad53 phosphorylation is. The simplest explanation for these results is that the low level of residual Rad53 phosphorylation seen in *mec1Δ* mutants is sufficient to at least partially regulate transcriptional but not other checkpoint responses. As such, this study provides a more comprehensive network of the checkpoint-kinase-mediated transcriptional response than the Mec1-mediated response previously reported by Gasch et al. (2001).

The observation that deletion of *MEC1* or *DUN1* had similar effects on differential gene expression in response to MMS treatment is consistent with previous results by Gasch et al. (2001). One possible explanation for this observation is that activation of Dun1 by Rad53 is solely Mec1 dependent (Tel1 cannot compensate for the loss of Mec1). Possible explanations for this would be that activation of Dun1 by Rad53 might require a scaffold containing Mec1 or that the interaction between Rad53 and Dun1 might require phosphorylation of at least one of these proteins by Mec1 specifically. Dun1 does contain a consensus site (S176) for Mec1/Tel1 that is phosphorylated in vivo and can serve as a substrate for Mec1 phosphorylation in vitro (Albuquerque et al., 2008; Mallory et al., 2003). Mutation of this site and the two other Mec1/Tel1 consensus sites on Dun1 did not cause the increased MMS sensitivity caused by deletion of *DUN1*; however, Mec1 and Tel1 were still able to phosphorylate this mutant to a lesser extent in vitro, suggesting the existence of additional Mec1/Tel1 phosphorylation sites (Mallory et al., 2003). These observations suggest that activation of Dun1 is more complex than a linear Mec1 > Rad53 > Dun1 pathway.

The fact that most of the TFs predicted to act downstream of Rad53 were phosphorylated in a Rad53-dependent manner suggests that they are regulated by phosphorylation. Although

much of this regulation may be due to phosphorylation by Rad53, phosphorylation by Dun1 is also Rad53 dependent (Allen et al., 1994). Thus, the phosphorylation sites identified on TFs in the Dun1-dependent transcriptional response are likely regulated by Dun1. Another possibility is that other kinases or phosphatases downstream of Rad53 and Dun1 may be responsible for phosphorylation of the TFs. In fact, a number of Rad53-dependent sites observed did not fit Rad53 or Dun1 consensus phosphorylation sites or Mec1/Tel1 consensus phosphorylation sites (Table 1). We also observed Rad53-dependent dephosphorylation at sites on several TFs, presumably mediated by activation of downstream phosphatases or inhibition of downstream kinases, suggesting alternative mechanisms for indirect phosphoregulation of TFs by Rad53. Although beyond the scope of this study, the effects of mutating these phosphorylation sites on MMS-induced transcriptional profiles in future experiments will better delineate the mechanisms by which the checkpoint kinases regulate TFs.

Nearly 900 genes were differentially expressed in response to MMS independently of the checkpoint kinase cascade, and ~300 of these checkpoint-kinase-independent genes were predicted to be targets of a distinct network of TFs (Hsf1, Hap1, Hap4, Rcs1, Rpn4, Sut1, Yap1, and Yap7). Direct analysis of the nonessential TFs in this network confirmed that they regulate expression of checkpoint-kinase-independent genes but also revealed that they regulate checkpoint-kinase-dependent genes (Figures 6B, S8, S9, and S10). Most of the kinase-dependent genes showing reduced differential expression in these TF mutants were not predicted targets of the corresponding TFs in the Beyer et al. analysis (Beyer et al., 2006). Because this analysis incorporated ChIP-Chip and predicted TF recognition site data to assign direct TF target predictions, the simplest explanation for this finding is that these checkpoint-kinase-dependent genes are regulated indirectly by these TFs.

A previous study identified genes that showed Mec1- and Dun1-independent regulation in response to MMS but likely misclassified many checkpoint-kinase-dependent genes as checkpoint-kinase-independent because, unlike our study, *rad53Δ* and *mec1Δ tel1Δ* mutants were not analyzed (Gasch et al., 2001). Although we have not ruled out the possibility that there could be some checkpoint-independent genes that are regulated redundantly by the Chk kinases (Rad53, Dun1, and Chk1) and, thus, only revealed by analyzing a *rad53Δ dun1Δ chk1Δ* triple mutant, these kinases should all be downstream of Mec1 and Tel1. That study also mentioned that a small number of Mec1- and Dun1-independent genes were shown to be targets of Yap1, Hsf1, and Hap1 in other studies. In contrast, our enrichment analysis provides a more rigorous systematic approach for identifying specific TFs downstream of both the checkpoint-kinase-dependent and -independent damage responses and has implicated many more TFs in the DDR than previously appreciated. Specifically, we found that Hsf1, Rcs1, and Yap1 targets involved in stress responses were primarily upregulated in response to MMS, whereas targets of Hap1 and Hap4 involved in oxidation reduction were primarily downregulated. Gasch et al. also observed that known Yap1 and Hap1 targets were differentially expressed in response to MMS but not ionizing radiation and that potential Hsf1 targets were upregulated by MMS but downregulated by ionizing radiation and suggested that the MMS-induced, Mec1-independent transcriptional response was not specific for DNA damage but rather was a consequence of cellular oxidative stress induced by MMS treatment (Gasch et al., 2001). Given our observation that the checkpoint-kinase-independent transcriptional response also involves TFs that participate in stress responses (Msn4 and Gcn4, Figure 3C), it seems probable that MMS induces gene expression changes associated with general stress responses in parallel with those associated with the DDR. Future studies using a diversity of DNA-damaging agents and involving direct analysis of individual TFs should more precisely define the components of the kinase-independent gene expression network that are DNA damage induced and those that are nonspecific stress responses.

## EXPERIMENTAL PROCEDURES

### *S. cerevisiae* Strains

The strains used in the expression-profiling experiments were Mat-a strains derived either from the *S. cerevisiae* knockout collection or from BY4741 (YSC1053; Open Biosystems, Thermo Scientific) using standard gene knockout methods. WT (*sml1Δ*) and *rad53Δsml1Δ* versions of arginine plus lysine auxotrophic strains containing TAP-tagged TFs were used for the SILAC experiments. All strains are listed in Table S1.

### Gene Expression Profiling

The gene expression experiments were carried out as described previously (Workman et al., 2006) using Agilent microarrays (Yeast v.2). Two independent experiments comparing MMS-treated (0.03%) with untreated cells were performed on two independent isolates for each strain.

### Processing and Analysis of Expression Array Data

The median intensities of technically replicated probes were analyzed with the *LinearModels of Microarray data* package (LIMMA) (Smyth, 2005). LIMMA was also employed to compare and detect significant differences in differential expression between the kinase or TF deletion and WT strains for each gene. Data are included in Table S2 and summarized in Table S3.

### Enrichment Analysis

The sets of genes that were categorized as kinase dependent (i.e., genes with significantly reduced differential expression in each mutant; Figure 3C; Table S6), as genes that were kinase dependent in at least two of the experiments (the checkpoint-kinase-dependent set; Figure 6A; Table S10), or as genes that were not kinase dependent in any experiment (the checkpoint-kinase-independent set; Figure 6A; Table S10) were evaluated for enrichment of targets of each TF (Beyer et al., 2006) using the hypergeometric test. Enrichment analysis for cell-cycle-regulated genes (Figures 5A and 5B; Table S9) was executed by evaluating the sets of Rad53-dependent up- and downregulated genes (both all Rad53-dependent genes and genes that are targets of a given TF) were instead evaluated for enrichment with genes having peak expression at the specified cell-cycle stages (Spellman et al., 1998).

### FACS

Asynchronous cultures were grown using the same conditions used for the microarray experiment. For synchronized cell-cycle experiments, cultures were arrested in G1 with 5 μg/ml α factor (AnaSpec), washed, and incubated in YPD containing 20 μg/ml nocodazole and 100 μg/ml pronase E (Sigma-Aldrich) with or without 0.03% MMS. Cells were stained with 1 μM SYTOX Green (Invitrogen) and analyzed by FACS.

### Identification of Rad53-Dependent Phosphorylation Sites by SILAC

Cultures of WT and *rad53Δ* strains with TAP-tagged TFs were grown in synthetic media supplemented with amino acids including either normal “light” L-arginine and L-lysine or deuterium-labeled “heavy” L-arginine and L-lysine (L-Arginine-<sup>13</sup>C<sub>6</sub>,<sup>15</sup>N<sub>4</sub> hydrochloride [608033] and L-Lysine-<sup>13</sup>C<sub>6</sub>,<sup>15</sup>N<sub>2</sub> hydrochloride [608041] from Sigma-Aldrich) as described previously by Chen et al. (2010). After treatment with 0.03% MMS for 1 hr, equal amounts of both cultures were combined, the TAP-tagged TF was purified, digested with trypsin, enriched for phosphopeptides by IMAC (Stensballe and Jensen, 2004), and analyzed by MS-MS. The data for peaks identified as peptides from each TF are shown in Table S8. See Extended Experimental Procedures for detailed Experimental Procedures.

## Supplementary Material

Refer to Web version on PubMed Central for supplementary material.

## Acknowledgments

The authors would like to thank R.D.K. and T.G.I. lab members for helpful discussions and the Huilin Zhou lab for help with the mass spectrometry experiments. This work was supported by NIH grants F32 GM086899 (to E.J.J.), ES014811 (to T.G.I.), GM26017 (to R.D.K.), and GM085764 (to T.G.I.).

## REFERENCES

- Albuquerque CP, Smolka MB, Payne SH, Bafna V, Eng J, Zhou H. A multidimensional chromatography technology for in-depth phosphoproteome analysis. *Mol. Cell. Proteomics*. 2008; 7:1389–1396. [PubMed: 18407956]
- Allen JB, Zhou Z, Siede W, Friedberg EC, Elledge SJ. The SAD1/RAD53 protein kinase controls multiple checkpoints and DNA damage-induced transcription in yeast. *Genes Dev*. 1994; 8:2401–2415. [PubMed: 7958905]
- Bähler J. Cell-cycle control of gene expression in budding and fission yeast. *Annu. Rev. Genet*. 2005; 39:69–94. [PubMed: 16285853]
- Bardwell L. A walk-through of the yeast mating pheromone response pathway. *Peptides*. 2004; 25:1465–1476. [PubMed: 15374648]
- Bashkirov VI, Bashkirova EV, Haghazari E, Heyer WD. Direct kinase-to-kinase signaling mediated by the FHA phosphoprotein recognition domain of the Dun1 DNA damage checkpoint kinase. *Mol. Cell. Biol*. 2003; 23:1441–1452. [PubMed: 12556502]
- Basrai MA, Velculescu VE, Kinzler KW, Hieter P. NORF5/HUG1 is a component of the MEC1-mediated checkpoint response to DNA damage and replication arrest in *Saccharomyces cerevisiae*. *Mol. Cell. Biol*. 1999; 19:7041–7049. [PubMed: 10490641]
- Bastos de Oliveira FM, Harris MR, Brazauskas P, de Bruin RA, Smolka MB. Linking DNA replication checkpoint to MBF cell-cycle transcription reveals a distinct class of G1/S genes. *EMBO J*. 2012; 31:1798–1810. [PubMed: 22333912]
- Beyer A, Workman C, Hollunder J, Radke D, Möller U, Wilhelm T, Ideker T. Integrated assessment and prediction of transcription factor binding. *PLoS Comput. Biol*. 2006; 2:e70. [PubMed: 16789814]
- Branzei D, Foiani M. The Rad53 signal transduction pathway: replication fork stabilization, DNA repair, and adaptation. *Exp. Cell Res*. 2006; 312:2654–2659. [PubMed: 16859682]
- Branzei D, Foiani M. The checkpoint response to replication stress. *DNA Repair (Amst.)*. 2009; 8:1038–1046. [PubMed: 19482564]
- Chen SH, Albuquerque CP, Liang J, Suhandynata RT, Zhou H. A proteome-wide analysis of kinase-substrate network in the DNA damage response. *J. Biol. Chem*. 2010; 285:12803–12812. [PubMed: 20190278]
- Gasch AP, Huang M, Metzner S, Botstein D, Elledge SJ, Brown PO. Genomic expression responses to DNA-damaging agents and the regulatory role of the yeast ATR homolog Mec1p. *Mol. Biol. Cell*. 2001; 12:2987–3003. [PubMed: 11598186]
- Ghavidel A, Kislinger T, Pogoutse O, Sopko R, Jurisica I, Emili A. Impaired tRNA nuclear export links DNA damage and cell-cycle check-point. *Cell*. 2007; 131:915–926. [PubMed: 18045534]
- Hinnebusch AG, Fink GR. Positive regulation in the general amino acid control of *Saccharomyces cerevisiae*. *Proc. Natl. Acad. Sci. USA*. 1983; 80:5374–5378. [PubMed: 6351059]
- Huang M, Zhou Z, Elledge SJ. The DNA replication and damage checkpoint pathways induce transcription by inhibition of the Crt1 repressor. *Cell*. 1998; 94:595–605. [PubMed: 9741624]
- Hutchins JR, Hughes M, Clarke PR. Substrate specificity determinants of the checkpoint protein kinase Chk1. *FEBS Lett*. 2000; 466:91–95. [PubMed: 10648819]

- Ideker T, Thorsson V, Ranish JA, Christmas R, Buhler J, Eng JK, Bumgarner R, Goodlett DR, Aebersold R, Hood L. Integrated genomic and proteomic analyses of a systematically perturbed metabolic network. *Science*. 2001; 292:929–934. [PubMed: 11340206]
- Kim ST, Lim DS, Canman CE, Kastan MB. Substrate specificities and identification of putative substrates of ATM kinase family members. *J. Biol. Chem.* 1999; 274:37538–37543. [PubMed: 10608806]
- Kim EM, Jang YK, Park SD. Phosphorylation of Rph1, a damage-responsive repressor of PHR1 in *Saccharomyces cerevisiae*, is dependent upon Rad53 kinase. *Nucleic Acids Res.* 2002; 30:643–648. [PubMed: 11809875]
- Koch C, Moll T, Neuberger M, Ahorn H, Nasmyth K. A role for the transcription factors Mbp1 and Swi4 in progression from G1 to S phase. *Science*. 1993; 261:1551–1557. [PubMed: 8372350]
- Kolodner RD, Putnam CD, Myung K. Maintenance of genome stability in *Saccharomyces cerevisiae*. *Science*. 2002; 297:552–557. [PubMed: 12142524]
- Liu Y, Vidanes G, Lin YC, Mori S, Siede W. Characterization of a *Saccharomyces cerevisiae* homologue of *Schizosaccharomyces pombe* Chk1 involved in DNA-damage-induced M-phase arrest. *Mol. Gen. Genet.* 2000; 262:1132–1146. [PubMed: 10660074]
- Mallory JC, Bashkurov VI, Trujillo KM, Solinger JA, Dominska M, Sung P, Heyer WD, Petes TD. Amino acid changes in Xrs2p, Dun1p, and Rfa2p that remove the preferred targets of the ATM family of protein kinases do not affect DNA repair or telomere length in *Saccharomyces cerevisiae*. *DNA Repair (Amst.)*. 2003; 2:1041–1064. [PubMed: 12967660]
- Morrow DM, Tagle DA, Shiloh Y, Collins FS, Hieter P. TEL1, an *S. cerevisiae* homolog of the human gene mutated in ataxia telangiectasia, is functionally related to the yeast checkpoint gene MEC1. *Cell*. 1995; 82:831–840. [PubMed: 7545545]
- Paulovich AG, Hartwell LH. A checkpoint regulates the rate of progression through S phase in *S. cerevisiae* in response to DNA damage. *Cell*. 1995; 82:841–847. [PubMed: 7671311]
- Pramila T, Wu W, Miles S, Noble WS, Breeden LL. The Fork-head transcription factor Hcm1 regulates chromosome segregation genes and fills the S-phase gap in the transcriptional circuitry of the cell cycle. *Genes Dev.* 2006; 20:2266–2278. [PubMed: 16912276]
- Putnam CD, Jaehnig EJ, Kolodner RD. Perspectives on the DNA damage and replication checkpoint responses in *Saccharomyces cerevisiae*. *DNA Repair (Amst.)*. 2009; 8:974–982. [PubMed: 19477695]
- Rouse J, Jackson SP. Interfaces between the detection, signaling, and repair of DNA damage. *Science*. 2002; 297:547–551. [PubMed: 12142523]
- Sanchez Y, Desany BA, Jones WJ, Liu Q, Wang B, Elledge SJ. Regulation of RAD53 by the ATM-like kinases MEC1 and TEL1 in yeast cell cycle checkpoint pathways. *Science*. 1996; 271:357–360. [PubMed: 8553072]
- Sanchez Y, Zhou Z, Huang M, Kemp BE, Elledge SJ. Analysis of budding yeast kinases controlled by DNA damage. *Methods Enzymol.* 1997; 283:398–410. [PubMed: 9251037]
- Sanchez Y, Bachant J, Wang H, Hu F, Liu D, Tetzlaff M, Elledge SJ. Control of the DNA damage checkpoint by chk1 and rad53 protein kinases through distinct mechanisms. *Science*. 1999; 286:1166–1171. [PubMed: 10550056]
- Sidorova J, Breeden L. Analysis of the SWI4/SWI6 protein complex, which directs G1/S-specific transcription in *Saccharomyces cerevisiae*. *Mol. Cell. Biol.* 1993; 13:1069–1077. [PubMed: 8423776]
- Sidorova JM, Breeden LL. Rad53-dependent phosphorylation of Swi6 and down-regulation of CLN1 and CLN2 transcription occur in response to DNA damage in *Saccharomyces cerevisiae*. *Genes Dev.* 1997; 11:3032–3045. [PubMed: 9367985]
- Sidorova JM, Breeden LL. Rad53 checkpoint kinase phosphorylation site preference identified in the Swi6 protein of *Saccharomyces cerevisiae*. *Mol. Cell. Biol.* 2003; 23:3405–3416. [PubMed: 12724400]
- Smolka MB, Albuquerque CP, Chen SH, Zhou H. Proteome-wide identification of in vivo targets of DNA damage checkpoint kinases. *Proc. Natl. Acad. Sci. USA*. 2007; 104:10364–10369. [PubMed: 17563356]

- Smyth, GK. Limma: linear models for microarray data. In: Gentleman, RVC.; Dudoit, S.; Irizarry, R.; Huber, W., editors. *Bioinformatics and Computational Biology Solutions using R and Bioconductor*. New York: Springer; 2005. p. 397-420.
- Songyang Z, Blechner S, Hoagland N, Hoekstra MF, Piwnica-Worms H, Cantley LC. Use of an oriented peptide library to determine the optimal substrates of protein kinases. *Curr. Biol.* 1994; 4:973–982. [PubMed: 7874496]
- Spellman PT, Sherlock G, Zhang MQ, Iyer VR, Anders K, Eisen MB, Brown PO, Botstein D, Futcher B. Comprehensive identification of cell cycle-regulated genes of the yeast *Saccharomyces cerevisiae* by microarray hybridization. *Mol. Biol. Cell.* 1998; 9:3273–3297. [PubMed: 9843569]
- Stensballe A, Jensen ON. Phosphoric acid enhances the performance of Fe(III) affinity chromatography and matrix-assisted laser desorption/ionization tandem mass spectrometry for recovery, detection and sequencing of phosphopeptides. *Rapid Commun. Mass Spectrom.* 2004; 18:1721–1730. [PubMed: 15282771]
- Travesa A, Kuo D, de Bruin RA, Kalashnikova TI, Guaderrama M, Thai K, Aslanian A, Smolka MB, Yates JR 3rd, Ideker T, Wittenberg C. DNA replication stress differentially regulates G1/S genes via Rad53-dependent inactivation of Nrm1. *EMBO J.* 2012; 31:1811–1822. [PubMed: 22333915]
- Van Driessche N, Demsar J, Booth EO, Hill P, Juvan P, Zupan B, Kuspa A, Shaulsky G. Epistasis analysis with global transcriptional phenotypes. *Nat. Genet.* 2005; 37:471–477. [PubMed: 15821735]
- Verma R, Patapoutian A, Gordon CB, Campbell JL. Identification and purification of a factor that binds to the Mlu I cell cycle box of yeast DNA replication genes. *Proc. Natl. Acad. Sci. USA.* 1991; 88:7155–7159. [PubMed: 1871128]
- Verma R, Smiley J, Andrews B, Campbell JL. Regulation of the yeast DNA replication genes through the Mlu I cell cycle box is dependent on SWI6. *Proc. Natl. Acad. Sci. USA.* 1992; 89:9479–9483. [PubMed: 1409658]
- Workman CT, Mak HC, McCuine S, Tagne JB, Agarwal M, Ozier O, Begley TJ, Samson LD, Ideker T. A systems approach to mapping DNA damage response pathways. *Science.* 2006; 312:1054–1059. [PubMed: 16709784]
- Yoon S, Govind CK, Qiu H, Kim SJ, Dong J, Hinnebusch AG. Recruitment of the ArgR/Mcm1p repressor is stimulated by the activator Gcn4p: a self-checking activation mechanism. *Proc. Natl. Acad. Sci. USA.* 2004; 101:11713–11718. [PubMed: 15289616]

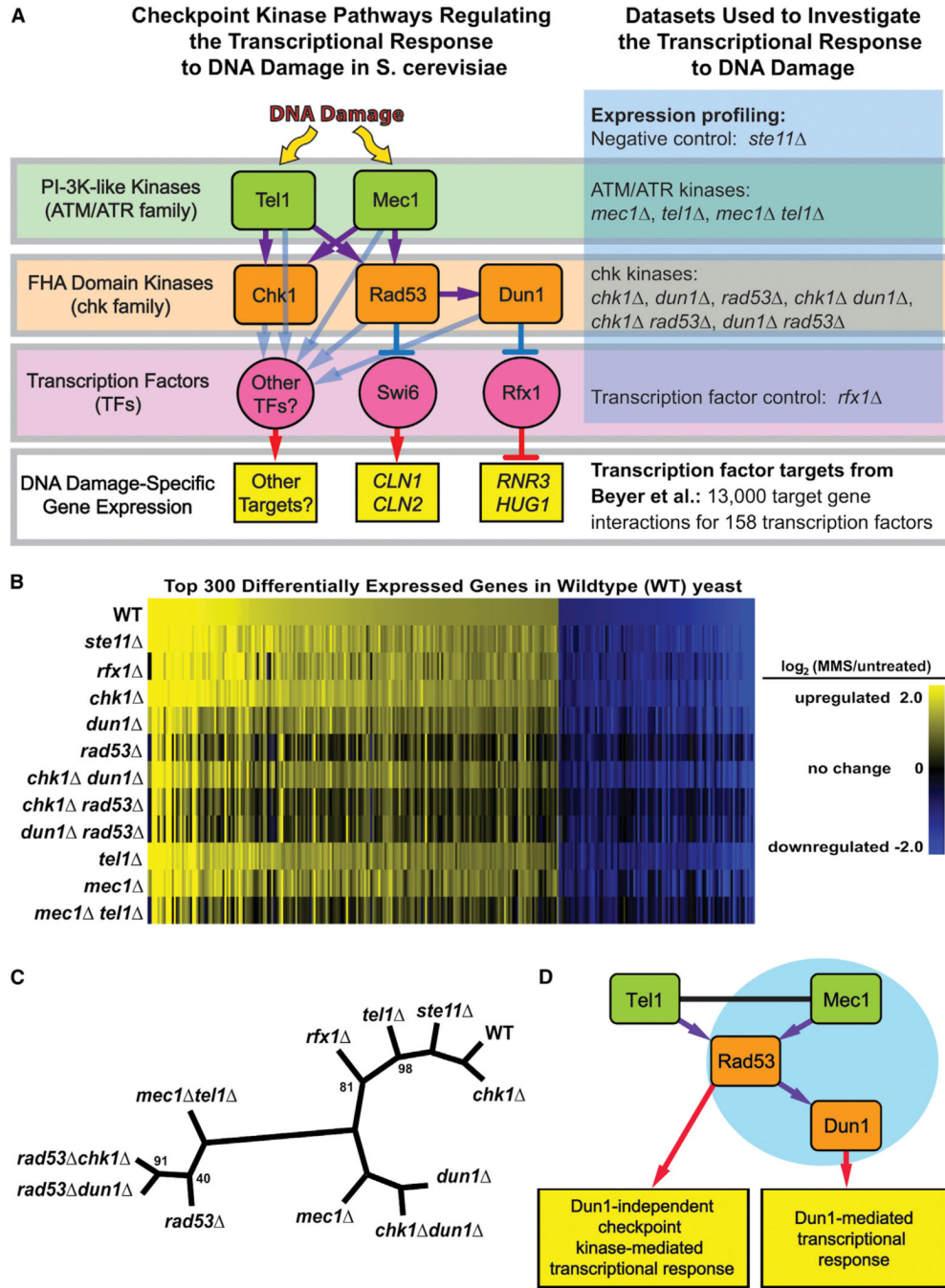


**Figure 1. Regulation of the Transcriptional Response to DNA Damage by the Checkpoint Kinase Signaling Cascade**

(A) Model for the regulation of transcription by the DNA damage checkpoint kinases (left) and overview of the data sets analyzed (right).

(B) MMS-induced changes in expression for each strain are shown here as vertical bars representing the log ratios (base 2) of gene expression in MMS-treated relative to untreated yeast for each of the 300 most differentially expressed genes in WT. Complete analysis of differential expression is provided in Table S2.

(C) Hierarchical clustering tree showing the Euclidean distance between the gene expression profiles of all the checkpoint kinase mutants. Clustering of the sample tree was bootstrapped (100 iterations); branch points with bootstrap values <100% are labeled.

(D) The refined model for the checkpoint-kinase-mediated transcriptional response indicates that the checkpoint-kinase-dependent transcriptional response to MMS treatment is primarily mediated by activation of Rad53 by Mec1 and Tel1 and that the Dun1-dependent transcriptional response represents a subset of the overall response. The blue circle indicates that the Dun1-dependent response is similar to Mec1-dependent response. See also Table S2.



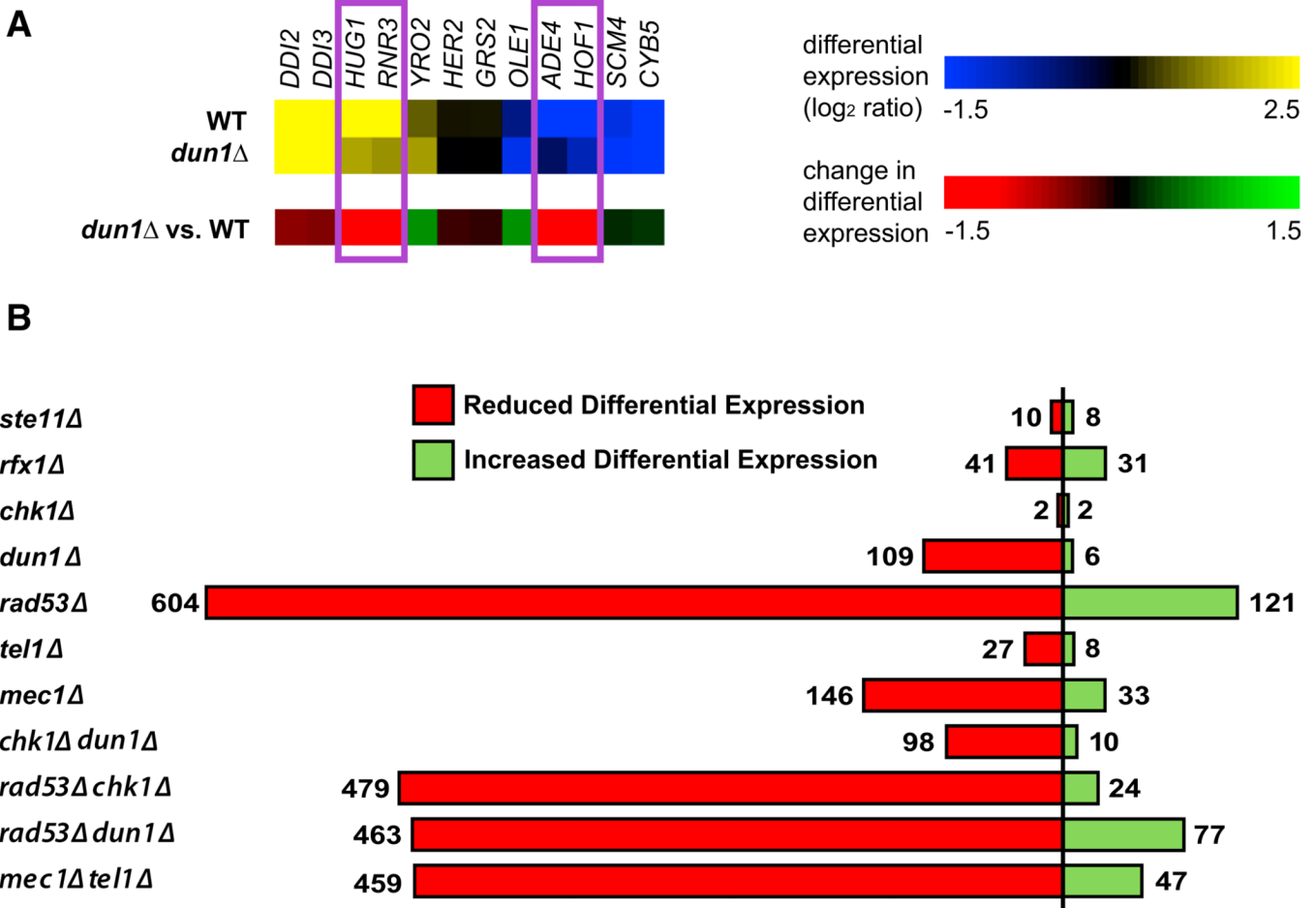


**Figure 2. Identification of Genes Showing Checkpoint-Kinase-Dependent Differential Expression**  
 (A) Example showing how deletion of *DUN1* affects DNA damage-induced changes in gene expression. The top panel shows gene expression of a selected set of genes from WT and the *dun1Δ* mutant strain, whereas the bottom panel (mutant versus WT) shows the effect of deleting the kinase on changes in gene expression.  
 (B) Bar graph of the total number of genes for which deleting the indicated kinase results in a statistically significant effect on DNA damage-induced differential expression. The relevant data are presented in Tables S2 and S3. See also Tables S2, S3, S4, and S5.

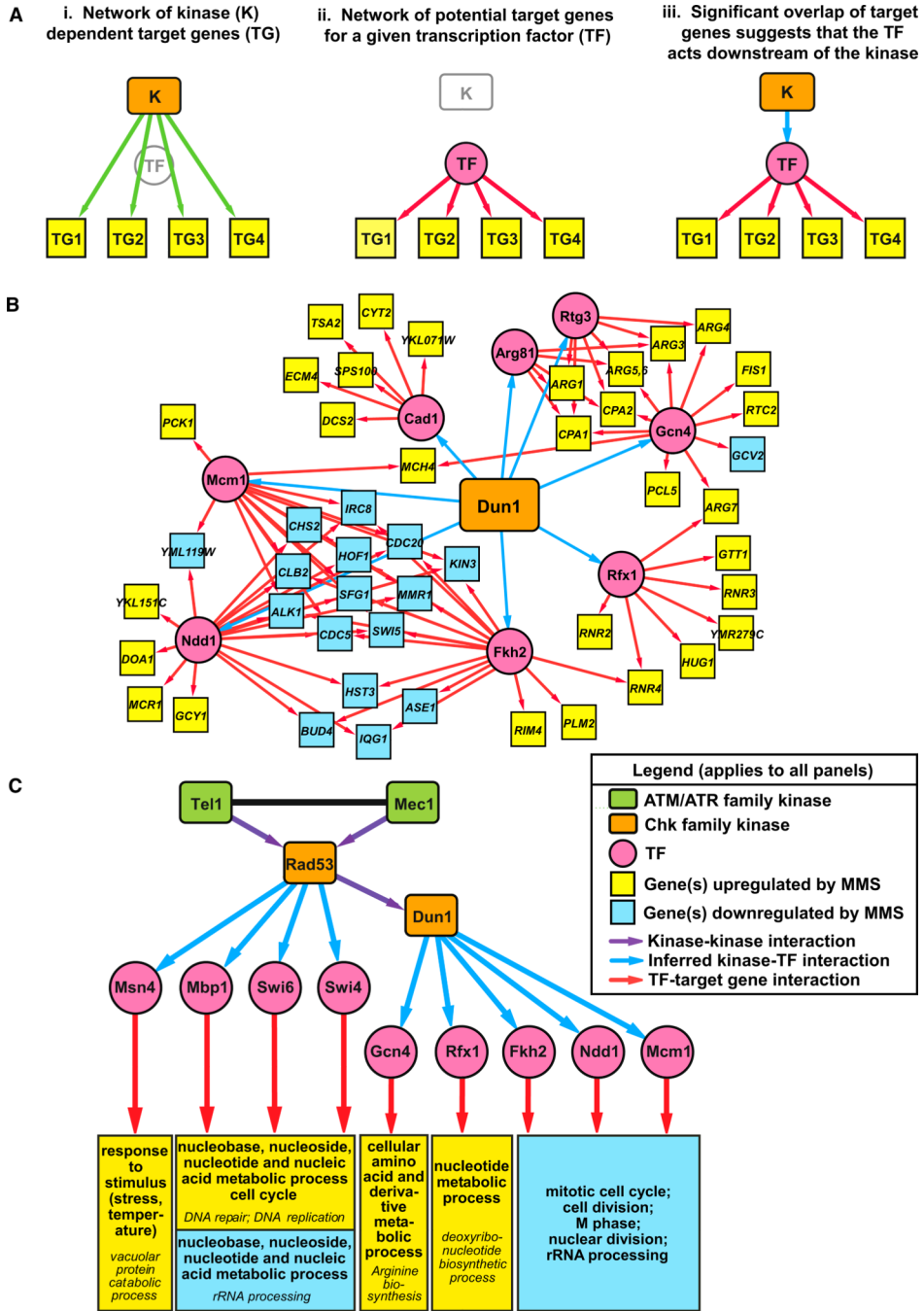


**Figure 3. Implicating TFs as Downstream Effectors of the Checkpoint-Kinase-Dependent Transcriptional Response to DNA Damage**  
 (A) Strategy used to identify kinase-TF interactions. (i) The kinase transcriptional regulatory network consists of interactions between the kinase and the set of target genes with kinase-dependent changes in gene expression. (ii) The TF regulatory network consists of predicted interactions between TFs and their target genes (Beyer et al., 2006). (iii) Significant overlap of target genes in the kinase and TF regulatory networks suggests that an interaction between the kinase and TF explains how the kinase regulates transcription of its target genes.

(B) The transcriptional regulatory network generated by applying this analysis to the Dun1-dependent set of target genes.

(C) A global transcriptional regulatory network showing kinase-TF interactions mediating the checkpoint-kinase-dependent transcriptional response to DNA damage. Kinase-TF interactions were only included in this network if four of the seven checkpoint-kinase-dependent gene sets showed enrichment for targets of the TF (see Table S6 for enrichment analysis and Figure S1 for a larger network that includes TFs enriched in two or more kinase-dependent gene sets). For simplicity, the target genes were replaced with modules showing the enriched GO terms in the sets of Rad53-dependent genes predicted to be targets of the TF (selected from Table S7). Fkh2, Ndd1, and Mcm1 form a transcriptional complex, and Swi6 forms distinct transcriptional complexes with Mbp1 (MBF) and Swi4 (SBF). Therefore, the Fhh2/Ndd1/Mcm1 and MBF/SBF target genes are represented in overlapping modules of enriched GO terms (see Figure S2). Fkh1 was omitted because nearly all of its predicted targets comprise a subset of the target genes of the Fkh2/Ndd1/Mcm1 complex. GO terms in italics are subcategories of the main GO terms listed above. See also Tables S6 and S7 and Figures S1 and S2.

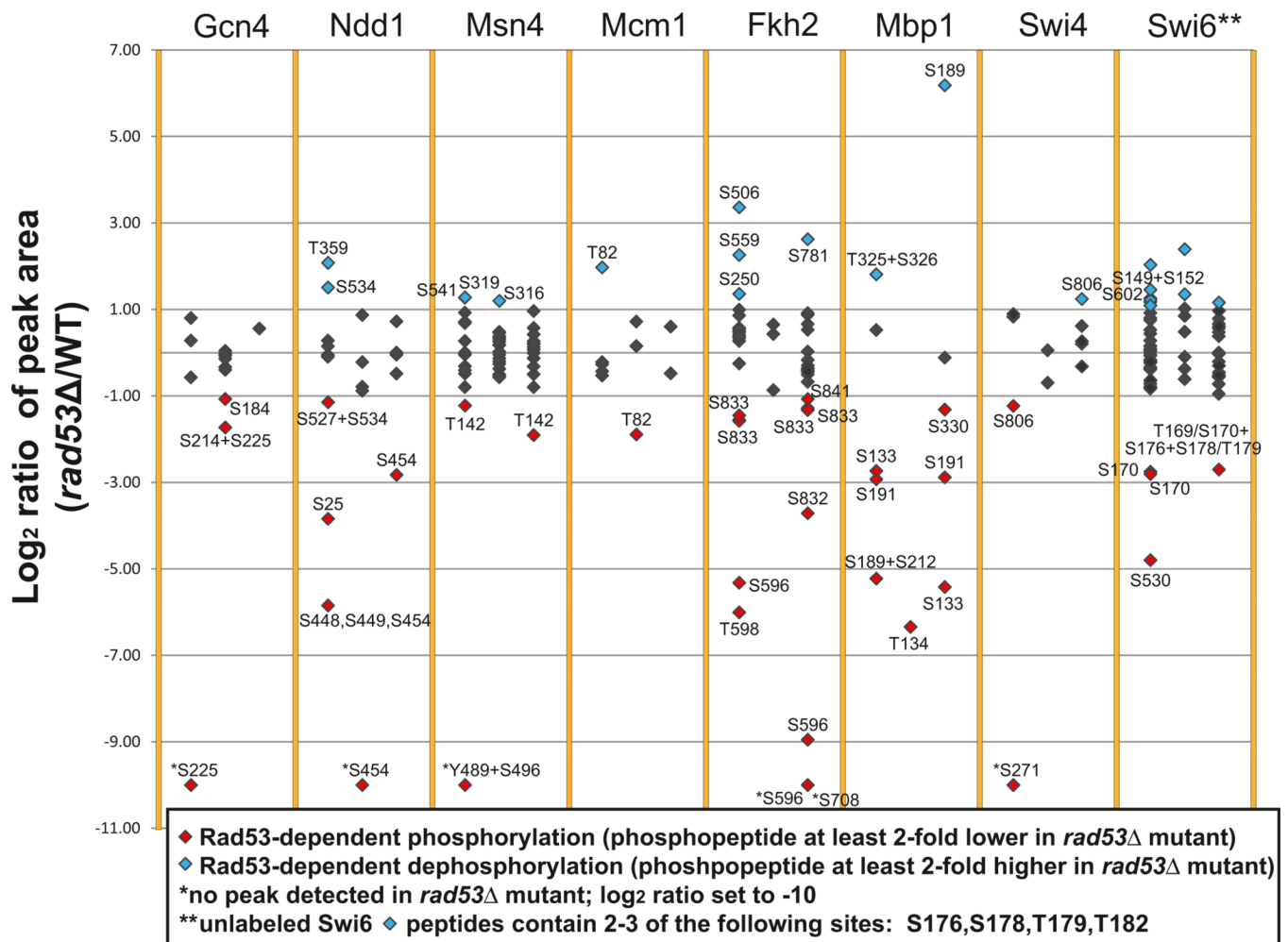


**Figure 4. Rad53-Dependent Phosphorylation of Downstream TFs**

The log<sub>2</sub> ratios obtained from SILAC analysis of the *rad53Δ* mutant relative to WT for each individual peak identifying a peptide with a phosphorylation site are shown. Data for each of three independent experiments are shown as adjacent scatterplots for each TF. Complete data for all of the peptides identified are presented in Table S8.

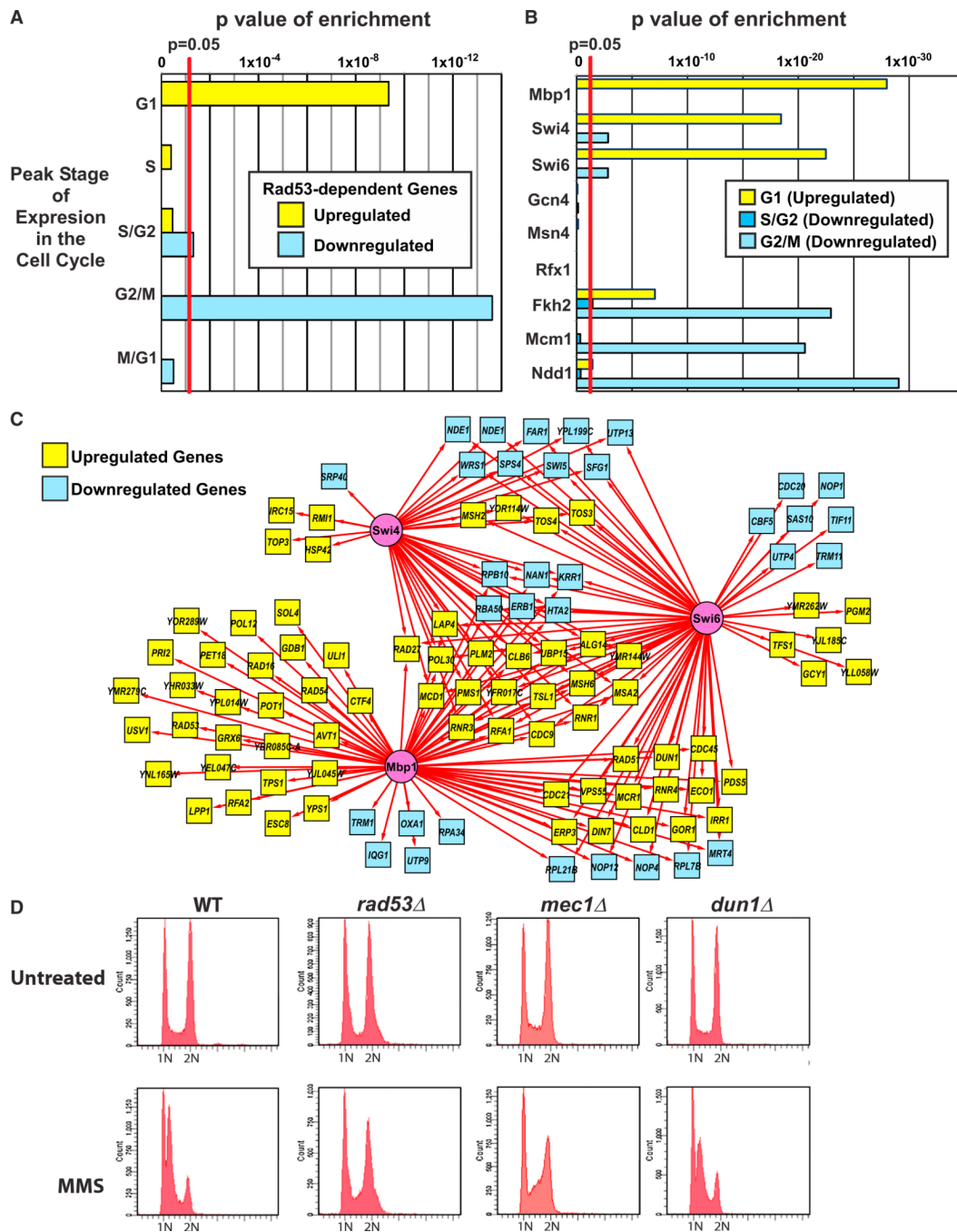


**Figure 5. Investigating the Relationship of the Checkpoint-Kinase-Dependent Transcriptional Response with the Cell Cycle**

(A) Checkpoint-kinase-dependent genes with peak expression in G1 phase are upregulated in response to MMS treatment, whereas genes with peak expression in S, G2, and M phases are downregulated. Graph shows p values for enrichment of genes reported to have peak expression at different stages of the cell cycle (Spellman et al., 1998) among the upregulated and downregulated sets of Rad53-dependent genes.

(B) Applying the same enrichment analysis for cell-cycle-specific expression to Rad53-dependent genes that are predicted targets of the TFs shown in Figure 3C reveals that upregulated targets of Mbp1, Swi4, Swi6, Fkh2, and Ndd1 are enriched for G1 genes,

downregulated targets of Fkh2 are enriched for S/G2 genes, and downregulated targets of Swi4, Swi6, Fkh2, Mcm1, and Ndd1 are enriched for G2/M genes (Table S9).

(C) The Rad53-dependent transcriptional regulatory network for predicted targets of Mbp1, Swi4, and Swi6.

(D) FACS analysis of asynchronous cultures of untreated and MMS-treated WT, *rad53* $\Delta$ , *mec1* $\Delta$ , and *dun1* $\Delta$  strains (see Figure S6 for other strains). See also Tables S4 and S9 and Figure S6.

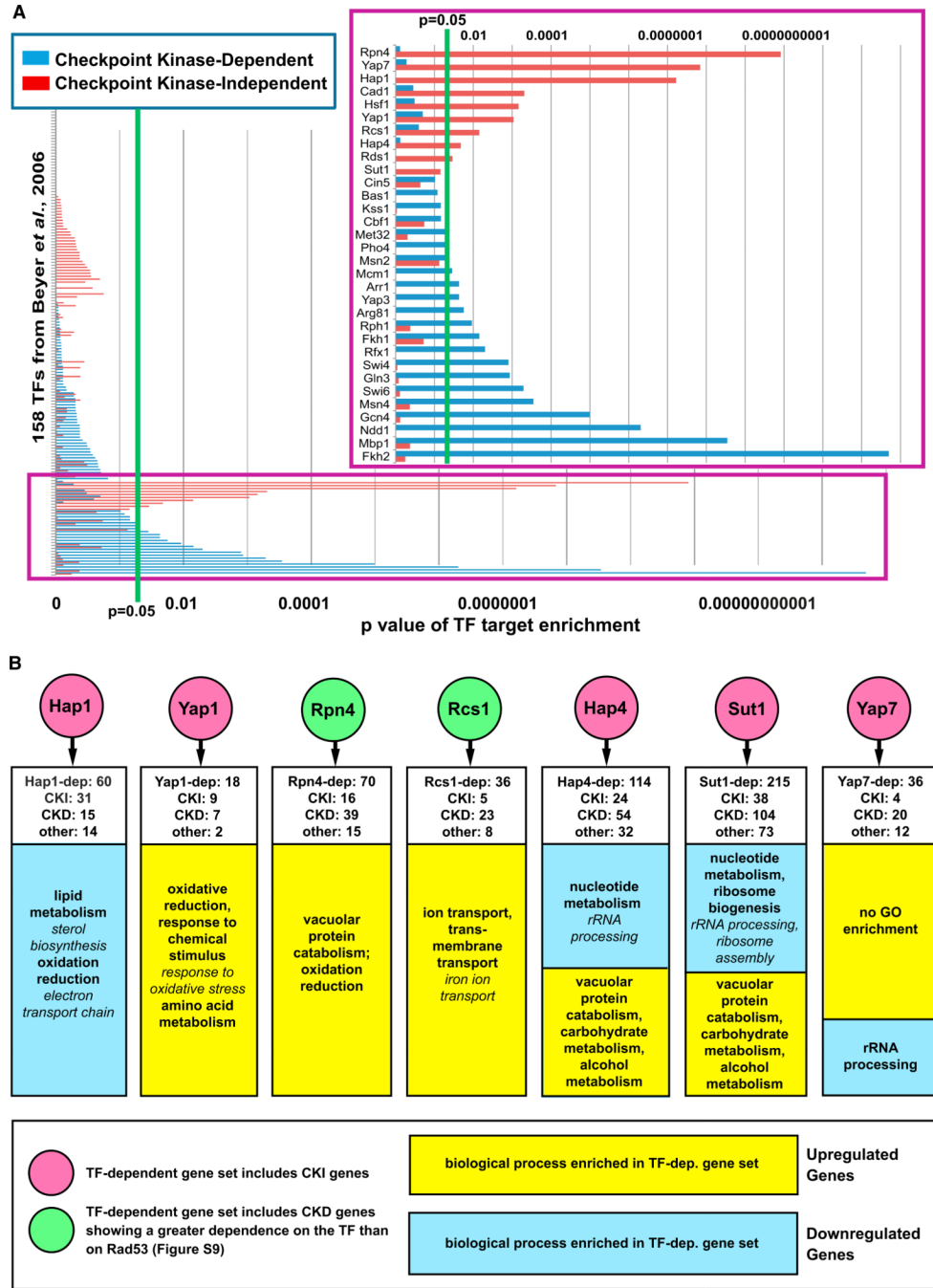


**Figure 6. Identification of TFs Mediating Checkpoint-Kinase-Independent Gene Expression in Response to MMS Treatment**

(A) The set of genes that was checkpoint kinase dependent (i.e., showed reduced differential expression in at least two of the checkpoint kinase mutants) and the set of genes that was checkpoint-kinase-independent (i.e., not affected by any of the checkpoint kinase mutations) show enrichment for targets of distinct sets of TFs. Enrichment for TF targets was performed as in Figure 3, and the p values for enrichment for targets of all 158 TFs are shown here and in Table S10. The inset shows TFs with enrichment p values that are <0.1. (B) Expression profiling confirms that the predicted TFs regulate checkpoint-kinase-independent (CKI) gene expression and identifies checkpoint-kinase-dependent (CKD)

genes regulated by the TFs (see Table S2 and Figures S8–S10 for expression profile data). TF-dependent genes for Hap1, Hap4, Rcs1, Sut1, and Yap7 were identified by expression profiling of TF mutants as in Figure 2 (see Table S3), whereas deletion-buffered genes from Workman et al. (2006) were analyzed for Rpn4 and Yap1. White boxes indicate the number of CKD and CKI genes that showed reduced differential expression in the TF mutant. GO terms in italics are subcategories of the main GO terms listed. See also Tables S2, S3, S4, S7, and S10 and Figure S7.



Table 1

Analysis of Rad53-Dependent Phosphorylation Sites Identified in Figure 4A

TF	Phosphosite <sup>a</sup>	Kinase Consensus Recognition	<i>rad53Δ</i> /WT <sup>c</sup>		
			Sequences <sup>b</sup>	Run 1	Run 2
Gen4	<b>S184</b>	Chk1; Rad53-A,C	ND	0.48	ND
Gen4	<b>S214</b>	Rad53-A	1.21	0.84	ND
Gen4	<b>S225</b>		0.00	0.78	ND
Gen4	<b>S214+S225</b>		ND	0.30	ND
Msn4	<b>T142</b>	Rad53-B	0.43	ND	0.27
Msn4	<b>S316</b>	Rad53-C	0.75	1.79	1.05
Msn4	<b>S319</b>		1.47	0.79	1.63
Msn4	<b>Y489</b>		0.56	1.24	0.71
Msn4	<b>S496</b>	Rad53-C	0.00	ND	ND
Msn4	<b>S541</b>		2.41	ND	ND
Msn4	<b>Y489+S496</b>		0.00	ND	ND
Fkh2	<b>S250</b>		2.56	ND	ND
Fkh2	<b>S506</b>	Mec1/Tel1	10.27	ND	ND
Fkh2	<b>S559</b>		1.81	ND	0.81
Fkh2	<b>S596</b>	Rad53-A,B	0.03	ND	0.00
Fkh2	<b>T598</b>		0.02	ND	ND
Fkh2	<b>S708</b>	Rad53-C	1.38	ND	0.67
Fkh2	<b>S714</b>		ND	ND	0.41
Fkh2	<b>S781</b>		ND	ND	6.16
Fkh2	<b>S832</b>	Rad53-B	1.37	1.57	1.61
Fkh2	<b>S833</b>	Rad53-C; Cdc28	0.59	1.36	0.43
Fkh2	<b>S841</b>		ND	ND	0.48
Mcm1	<b>T82</b>	Rad53-A; Mec1/Tel1	3.93	0.27	1.51
Ndd1	<b>S25</b>		0.07	ND	ND
Ndd1	<b>T359</b>	Rad53-C	4.22	ND	ND

TF	Phosphosite <sup>d</sup>	Kinase Consensus Recognition	<i>rad53ΔWTc</i>			
			Sequences <sup>b</sup>	Run 1	Run 2	Run 3
Ndd1	<b>S448</b>			0.02	ND	ND
Ndd1	<b>S449</b>		Rad53-B	0.02	ND	ND
Ndd1	<b>S454</b>		Rad53-A	0.02	0.00	0.14
Ndd1	<b>S527</b>		Rad53-A,C; Chk1; Dun1	1.20	0.58	1.03
Ndd1	<b>S534</b>			1.94	ND	ND
Ndd1	<b>S527+S534</b>			0.45	ND	ND
Mbp1	<b>S133</b>			0.15	ND	0.02
Mbp1	<b>T134</b>			ND	0.01	ND
Mbp1	<b>S189</b>		Mec1/Tel1	0.03	ND	72.72
Mbp1	<b>S191</b>		Chk1; Dun1	0.13	ND	0.14
Mbp1	<b>S212</b>		Rad53-A,B,C	0.03	ND	ND
Mbp1	<b>S330</b>		Rad53-B,C	ND	ND	0.40
Mbp1	<b>T325</b>			3.51	ND	ND
Mbp1	<b>S326</b>		Rad53-C	3.51	ND	ND
Mbp1	<b>S189+S212</b>			0.03	ND	ND
Mbp1	<b>T325+S326</b>			3.51	ND	ND
Swi4	<b>S271</b>		Rad53-A	0.00	ND	ND
Swi4	<b>S806</b>			0.43	1.04	2.36
Swi6	<b>S149</b>		Rad53-A	0.99	ND	0.52
Swi6	<b>S152</b>		Rad53-B	1.12	ND	0.52
Swi6	<b>T169</b>		Rad53-B,C	1.74	ND	0.15
Swi6	<b>S170</b>		Rad53-A,C	0.37	0.59	0.15
Swi6	<b>S176</b>			0.94	1.23	1.09
Swi6	<b>S178</b>			1.27	1.43	1.02
Swi6	<b>T179</b>			1.07	1.34	1.19
Swi6	<b>T182</b>			1.75	1.97	1.55
Swi6	<b>S530</b>			0.04	ND	ND
Swi6	<b>S602</b>			2.13	ND	ND

TF	Phosphosite <sup>a</sup>	Kinase Consensus Recognition	<i>rad53Δ</i> /WT <sup>c</sup>			
			Sequences <sup>b</sup>	Run 1	Run 2	Run 3
Swi6	<i>S149+S152</i>			1.62	ND	0.52
Swi6	<i>S176+T179</i>			1.32	1.58	1.24
Swi6	<b>T169+S176+T179</b>			ND	ND	0.15
Swi6	<b>S170+S176+S178</b>			0.79	0.65	0.15
Swi6	<i>S176+S178+T179</i>			2.74	2.31	1.65
Swi6	<i>S176+S178+T182</i>			ND	2.43	2.03
Swi6	<i>S176+T179+T182</i>			1.37	2.55	1.70
Swi6	<i>S178+T179+T182</i>			4.09	5.25	2.16

ND, phosphosite not detected or not quantifiable.

<sup>a</sup>Phosphorylation sites identified in Figure 4 as potentially phosphorylated (**bold**) or dephosphorylated (*italics*) in a Rad53-dependent manner or both (normal).

<sup>b</sup>Potential consensus sites for Rad53 are denoted as Rad53-A for the consensus sequence reported by Smolka et al. (2007), whereas sites characterized by Sidorova and Breeden are classified as either complete (Rad53-B,C) or as one-half sites as follows: Rad53-B is the one-half site amino terminal to the phosphosite, and Rad53-C is the one-half site carboxy-terminal to the phosphosite (Sidorova and Breeden, 2003). Consensus recognition sequences reported previously for Mec1/Tel1, Dun1, Chk2, and Cdc28 were used for this analysis (Hutchins et al., 2000; Kim et al., 1999; Sanchez et al., 1997; Songyang et al., 1994).

<sup>c</sup>For each experiment run, the total area of all the MS1 peaks corresponding to peptides with the phosphosite in the *rad53Δ* mutant was divided by the total area of the equivalent MS1 peaks in the WT strain and normalized to the median ratio for all peptides observed in the experiment.